



Elasmobranch vulnerability to global warming: insights from bioenergetic modelling of catsharks under climate scenarios

Noémie Coulon^{a,b,*}, Sophie Elliott^c, Thomas Barreau^d, Julie Lucas^a, Emma Gousset^a, Eric Feunteun^a, Alexandre Carpentier^e

^a Laboratoire de Biologie des Organismes et Ecosystèmes Aquatiques (BOREA) MNHN, CNRS, IRD, SU, UCN, UA, Dinard, France

^b UMR Marine Biodiversity, Exploitation and Conservation (MARBEC), Université de Montpellier, CNRS, IFREMER, IRD, Montpellier, France

^c Game & Wildlife Conservation Trust, Salmon & Trout Research Centre, East Stoke, Wareham BH20 6BB, United Kingdom

^d Service des stations marines, Station marine de Dinard, Dinard, France

^e Université de Rennes, Laboratoire de Biologie des Organismes et Ecosystèmes Aquatiques (BOREA) MNHN, CNRS, IRD, SU, UCN, UA, Rennes, France

ARTICLE INFO

Keywords:

Individual-based models
IPCC
Life history traits
Population dynamics
Shark
Temperature

ABSTRACT

Ectotherms are especially vulnerable to global warming due to their temperature-sensitive metabolic processes, impacting survival and reproductive success. Elasmobranchs, with slow life histories and low reproductive rates, may face amplified risks. In this study, we investigated two catshark species with distinct life traits and distributions: the Small-spotted Catshark (*Scyliorhinus canicula*) and the Nursehound (*S. stellaris*). Using newly calibrated bioenergetic models, we assessed changes in growth, sexual maturity, offspring production, and population dynamics under two CMIP6 climate scenarios projected for 2100: SSP2–4.5 (Middle of the Road) and SSP5–8.5 (Fossil-fueled Development), comparing these to historical data (1994–2015). Survival rates for early life stages remained similar under historical temperatures (80 %) and SSP2 (83 %) but dropped sharply under SSP5 to 33 % for *S. canicula* and 23 % for *S. stellaris*. Under both SSP2 and SSP5, *S. canicula* showed slight delays in maturation, yet the proportion of mature individuals ultimately exceeded historical levels in SSP2. Conversely, *S. stellaris* experienced progressively delayed maturation with warming. In SSP5, reduced growth, reproduction, and survival caused a population crash for *S. stellaris*, suggesting potential extinction. Our results reveal contrasting climate impacts on these species, underscoring the risk for late-maturing, low-fecundity, and narrowly distributed species. This emphasizes the urgency of conservation strategies tailored to mitigate their vulnerability to global warming.

1. Introduction

Global warming is causing rapid and widespread disruptions across all levels of biological organisation, from physiological processes (Little et al., 2020) and life history traits (Holt and Jørgensen, 2015; Huss et al., 2019) to population dynamics (Lindmark et al., 2022; Munday et al., 2008). Most teleost fish, being ectothermic, have metabolisms intrinsically tied to temperature variations (Lefevre et al., 2021; Schulte, 2015). Consequently, changes in survival rates due to metabolic constraints (Madeira et al., 2016) are among the first responses expected to directly and significantly impact population size. Additionally, surviving fish may experience altered growth and/or maturation due to the combined effects of thermal stress (Niu et al., 2023) and increased unpredictability in resource availability (Brodersen et al., 2011; Lindmark et al., 2022).

Population dynamics could either accelerate or slow down according to the temperatures experienced by individuals, the species' activity and reproductive strategies (Otero et al., 2012; Shapiro Goldberg et al., 2019). Lastly, considering that the physical condition of fish and water temperatures significantly impact the quantity and quality of their eggs and sperm (Baudron et al., 2014; Bobe and Labbé, 2010; Donelson et al., 2010; Pankhurst et al., 1996), variations in temperature could potentially influence the size of initial cohorts.

This is particularly concerning for elasmobranchs, which are late-maturing species with very low fecundity compared to teleost fish (Coulon et al., 2023). Given their slow rate of population renewal, the effects of climate change on elasmobranch population dynamics may not be fully realised until populations have already collapsed (i.e., time-lag effect). For example, bioenergetic model-based predictions by Lear et al.

* Corresponding author at: Université de Montpellier, Place Eugène Bataillon, 34090, Montpellier, France.

E-mail address: noemie.coulon@umontpellier.fr (N. Coulon).

<https://doi.org/10.1016/j.ecolmodel.2025.111157>

Received 6 November 2024; Received in revised form 4 April 2025; Accepted 19 April 2025

Available online 25 April 2025

0304-3800/© 2025 The Author(s). Published by Elsevier B.V. This is an open access article under the CC BY-NC license (<http://creativecommons.org/licenses/by-nc/4.0/>).

(2020) suggest that future increases in temperature regimes could severely affect the survival, growth and body condition of endangered Bull Shark (*Carcharhinus leucas*) and Largetooth Sawfish (*Pristis pristis*). Similarly, Neer et al. (2007) found that a 2 °C average temperature increase could delay the age at maturity of the American Cownose Ray (*Rhinoptera bonasus*) by 1–2 years, depending on its ability to meet increased energy requirements. Rising temperatures are expected to have a major impact on the embryos of oviparous species. Rising temperatures could significantly reduce their hatching success (Musa et al., 2020; Rosa et al., 2014), potentially dropping to only 11 % in a scenario where greenhouse gas emissions triple by 2075 (Coulon et al., 2024a). In the Northeast Atlantic, skates and sharks are particularly vulnerable due to the rapid warming of the North Sea and English Channel (Dulvy et al., 2008; Coulon et al., 2024b; Sgotti et al., 2016; Simon et al., 2023), to which is added substantial modern fishing efforts (Rousseau et al., 2019) and non-selective fishing techniques (Smith and Garcia, 2014; Walls and Dulvy, 2021).

The small-spotted catshark (*Scyliorhinus canicula*) is a demersal shark widely distributed across the Northeast Atlantic, ranging from the North Sea to the Bay of Biscay, and inhabits various depths from coastal waters to the deeper regions of the Celtic Sea. In contrast, Nursehound (*Scyliorhinus stellaris*), a shark with a similar lifestyle, is more commonly found in shallow waters around the British Isles (Bisch et al., 2024; Coulon et al., 2024b; Ellis et al., 2004). As a result, *S. canicula* experiences a broader temperature range (~10 °C to 17 °C) compared to *S. stellaris*. (~10 °C to 13 °C; Figure S1). These two catsharks also have markedly distinct life-history traits. *S. canicula* females mature before *S. stellaris* ones and produce three to six times more eggs (Ellis and Shackley, 1997; Ivory et al., 2004; Pecuchet et al., 2017). Conversely, *S. canicula* can reach a maximum size of up to 70 cm, which is half that of *S. stellaris* in this geographic region. Therefore, these disparities make *S. canicula* and *S. stellaris* prime candidates for evaluating the potential pressure of temperature rise on population dynamics driven by metabolic processes.

Bioenergetic models are powerful tools for assessing population dynamics (Boyd et al., 2020; Politikos et al., 2015a; 2015b) and species range (Duncan et al., 2020; Payne et al., 2016) by incorporating physiological constraints. By simulating temperature changes, these models provide insights into species' responses to climate change, highlighting potential impacts and adaptive plasticity (Christianson and Johnson, 2020; Holsman et al., 2019). Most bioenergetic models follow one of two approaches (see Brownscombe et al., 2022 for details). The first, exemplified by the Dynamic Energy Budget (DEB; Kooijman, 2010) and Physiological Energy Budget (PEB; Sibly et al., 2013) models are grounded in principles of chemistry, physics, and thermodynamics, aiming for a mechanistic description of bioenergetics (Boult et al., 2018; Boyd et al., 2020). The second approach relies on ecophysiological responses at the organism level to estimate the Scope For Growth (SFG) of individuals, based on a budget of ingested energy and metabolic costs derived from observed physiological responses like consumption and respiration rates (Winberg, 1956). The Wisconsin Energy Budget (WEB; Kitchell et al., 1974, 1977) is based on this SFG approach. WEB is particularly effective for assessing how environmental conditions affect individual growth and survival, providing precise predictions based on temperature or food availability variations (Cerino et al., 2013; Hartman and Jensen, 2017). The data required for this model is often more readily available or easier to measure than those needed for more complex models like DEB. This is especially relevant for elasmobranchs, where such information is limited. With a history of successful application and validation (Deslaurliers et al., 2017), the Wisconsin Energy Budget (WEB) model offers a credible and robust method for studying catsharks' responses to environmental changes and population dynamics with limited data.

We developed a bioenergetic model under Wisconsin formulation in conjunction with a population dynamic matrix model, to assess the impact of end-of-century temperature projections on (i) individual

growth, (ii) life history traits, and (iii) the population dynamics of *S. canicula* and *S. stellaris*. Our analysis encompassed three climate change scenarios, depicting future socio-economic trajectories and their potential implications for greenhouse gas emissions spanning from current to extreme conditions, as outlined by the Shared Socio-Economic Pathways (SSP) framework (IPCC, 2021). Beyond developing a bioenergetic model specific to *S. canicula* and adapting it to *S. stellaris*, this study aimed to test the hypothesis that species with slower life paces and narrower environmental tolerances exhibit greater sensitivity.

2. Material & methods

2.1. Temperature scenarios

The Intergovernmental Panel on Climate Change (IPCC) Sixth Assessment Report assessed projected climate outcomes of a set of five scenarios that are based on the framework of the SSPs (IPCC, 2021). In this study, we used Northeast Atlantic historical temperature data from 1994 to 2015 and future temperature projections for 2100 based on two scenarios from the CMIP6 climate model. We considered SSP2–4.5 (Middle of the Road) and SSP5–8.5 (Fossil-fuelled Development) climate scenarios. SSP2–4.5 represents a scenario where CO₂ emissions stabilise at current levels until 2050 and then gradually decline, though they do not reach net zero by 2100 (Fricko et al., 2017). In contrast, SSP5–8.5, characterised by a 'Fossil-fuelled Development' pathway, anticipates a dramatic increase in CO₂ emissions, which are projected to triple by 2075 (Kriegler et al., 2017). The monthly temperatures were obtained from forecasts for Western and Central Europe, and downloaded from <http://interactive-atlas.ipcc.ch> (Gutiérrez et al., 2021; Iturbide et al., 2021; Fig. 1).

2.2. Bioenergetic model parameters

Bioenergetic models under Wisconsin formulation (Hanson et al., 1997) use an energy balance equation in which each of the physiological processes (metabolism, wastes, and growth) is described by a set of functions that are regulated primarily by water temperature and body weight (Winberg, 1956). They can be used to estimate growth, linking fish physiology to environmental conditions and quantifying the relative importance of various environmental factors on individual growth (Hanson et al., 1997). Consumed energy is first allocated to metabolism,

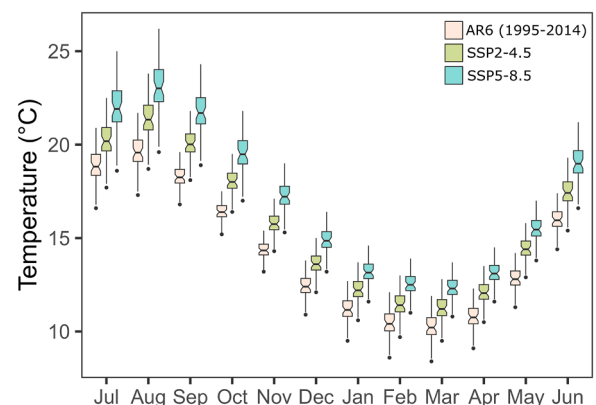




Fig. 1. Monthly water temperature applied to each individual. The temperatures were obtained from forecasts for Western and Central Europe and downloaded from <http://interactive-atlas.ipcc.ch> (Gutiérrez et al., 2021; Iturbide et al., 2021). Historical temperatures from 1994 to 2015 (AR6 1994–2015) are shown in beige. Temperatures predicted for 2100 under the climate scenarios SSP2–4.5 (Middle of the road) and SSP5 (Fossil-fuelled Development) are respectively shown in light green and light blue. The order of the months indicates the order of the temperatures experienced by the individuals during a simulation.

some is lost as waste and that left over can be allocated to growth.

The parameters for the bioenergetics models developed for *S. canicula* and *S. stellaris* follow the naming and parameter convention used in the Fish Bioenergetics 4.0 software (Deslauriers et al., 2017; Table 1). We tested multiple parameter combinations and report here those that allowed individuals under historical conditions to grow consistently with observed data for these two species. Maximum daily consumption (C_{max}) is expressed as a specific rate (g of prey consumed per g of body mass per day) and is estimated as an allometric function of

Table 1

Models and parameters used in the bioenergetic models for *S. canicula* and *S. stellaris*. Parameter names follow the convention of the Fish Bioenergetics 4.0 software (Deslauriers et al., 2017) under the Wisconsin Energy Budget formulation (Kitchell et al., 1974, 1977).

Model parameter	Explanation	<i>S. canicula</i>	<i>S. stellaris</i>
			
Consumption model equation		3	
CA	Intercept of the allometric mass function	0.0853	
CB	Slope of the allometric mass function	−0.15	
CQ	Lower water temperature where the temperature dependence is a small proportion (CK1) of C_{max}	9.7	10
CTO	Water temperature corresponding to 0.98 of C_{max}	11.3	11.4
CTM	Water temperature still corresponding to 0.98 of C_{max}	12.8	12
CTL	Upper water temperature where the temperature dependence is a small proportion (CK4) of C_{max}	18.5	
CK1	Small proportion of C_{max}	0.397	
CK4	Small proportion of C_{max}	0.655	
Respiration model equation		2	
RA	Intercept of the allometric mass function	0.000933	
RB	Slope of the allometric mass function	−0.0501	
RQ	Approximate the Q10 (the rate at which the function increases over relatively low water temperatures).	1.32	
RT0	Optimum temperature for respiration (where respiration is highest).	19	
RTM	Maximum (lethal) water temperature	21	
ACT	Activity multiplier	2.6 (Sims et al., 2006)	1.47 (Piiper et al., 1977)
SDA	Specific dynamic action	0.12 (Sims and Davies, 1994)	
Egestion model equation		1	
FA	Constant proportion of consumption	0.16	
Excretion model equation		1	
UA	Constant proportion of assimilated energy (consumption minus egestion)	0.1	

mass from *ad libitum* feeding experiments ranging from 0.07 of the weight of the smallest individuals to 0.03 of the weight of the largest (Neer et al., 2007), where CA and CB are the intercept and slope respectively.

$$C_{max} = CA \times W^{CB}$$

Maximum daily consumption was then modified by a temperature dependence function ($F(T)$) and a proportionality constant (p) that accounts for ecological constraints on the maximum feeding rate (C_{max}). The p value theoretically ranges from 0 to 1, with 0 representing no feeding, and 1 indicating the fish is feeding at its maximum rate based on its size and water temperature.

$$C = C_{max} \times p \times F(T)$$

The Thornton & Lessem (1978) model (consumption equation 3; Deslauriers et al., 2017) was used to describe the temperature dependence of C_{max} for each species ($F(T)$). This model provides a better fit for some cool- and coldwater species and is essentially the product of two sigmoid curves, one fit to the increasing portion of the temperature dependence function and the other to the decreasing portion. Records from the Ocean Biodiversity Information System (OBIS, 2023) openly available on <https://obis.org/>, were used to parametrize it (Figure S1, Table 1). Egestion (faecal waste, F) and excretion (nitrogenous waste, U) were computed as a constant proportion of consumed energy (Kitchell et al., 1977) (waste loss equation 1; Deslauriers et al., 2017). Specific rate of respiration (R) is dependent on individual mass (W), water temperature ($G(T)$) and an activity multiplier (ACT):

$$R = RA \times W^{RB} \times G(T) \times ACT$$

where RA and RB are the intercept and slope for the allometric mass function. RA and RB parameters for *S. canicula* were determined by Butler and Taylor (1975) but not using intermittent flow static respirometry method, commonly used method nowadays to measure standard metabolic rates (SMR)—the minimum oxygen consumption necessary for maintaining fundamental physiological functions such as respiration, blood circulation, and ion balance (Little et al., 2020). This method has been recognized as crucial and highly sensitive in bioenergetic models of fish (Bartell et al., 1986; Rice and Cochran, 1984). For this reason, we determined the relationship afresh by measuring standard metabolic rates and converting O_2 consumption rates ($g\ O_2\ g\ fish^{-1}\ day^{-1}$; Figure S2) using the oxy-calorific coefficient of $13,560\ J\ g\ O_2^{-1}$. Limited data on *S. stellaris* is available in the literature (Figure S2; Piiper et al., 1977). The O_2 consumption rates were not obtained using current methods and units, and we were unable to conduct additional laboratory measurements for this species. Therefore, we combined these data with those obtained experimentally for *S. canicula*. We determined a single model for both species, which was found to be similar to that defined for *S. canicula* alone (Figure S2). Consequently, the parameters characterising the specific rate of respiration of *S. canicula* were imputed to *S. stellaris*. The Kitchell et al. (1977) model (respiration equation 2; Deslauriers et al., 2017) was used to describe the temperature-dependence of respiration ($G(T)$) adjusted by an activity multiplier (ACT).

During calibration process, iterative simulations for 1000 females of *S. canicula* and *S. stellaris* were performed to adjust the p value for each age class (Deslauriers et al., 2017) until the daily growth simulated by the model resulted in a predicted weight at the end of each age that matched the observed weights at age determined from weight-length field data converted into weight-age data with the ‘fishR’ R package (Appendix 1). Weight-length field data were from the western part of the English Channel, the Irish Sea, the Celtic Sea and the Bay of Biscay. They included juveniles hatched at the Dinard marine station (Coulon et al., 2024a), females collected during the scientific bottom trawl surveys CAMANOC, EVHOE, and CGFS (Mahé et al., 2018), and females gathered from a survey at French fish auctions, Elasmobranch-on-Shore

(EOS), as part of the European Data Collection Framework, which aims to collect, analyse, and share data on elasmobranch fishing. Given that Von Bertalanffy growth parameters are highly dependent on the location of individuals, we used the parameters determined by Ivory & Nolan (2004) for females of *S. canicula* in the Irish Sea and the Celtic Sea ($L_{\infty, canicula} = 57$ cm; $Linf_{S, canicula} = 75.14$ cm; $K_{S, canicula} = 0.150$, $t_{0S, canicula} = -0.96$). Since the available growth parameters for *S. stellaris* are derived exclusively from Mediterranean individuals (Capapé et al., 2006), we used the growth parameters estimated using a von Bertalanffy growth model by Greenstreet et al. (2012) ($Linf_{S, stellaris} = 140$ cm; $K_{S, stellaris} = 0.094$, $t_{0S, stellaris} = -4.35$), that addressed redundancy in metrics describing the composition, structure, and functioning of the North Sea demersal fish community. However, the size at maturity reported in this study is questionable, as it is smaller than that observed in the Mediterranean (Finucci et al., 2021) although the size structure of *S. stellaris* in the North East Atlantic tends to present larger individuals (Bisch et al., 2024). Therefore, we considered as a proxy for the size at maturity, the smallest size female with an egg emerging from the cloaca observed opportunistically at fish auctions during EOS (Table S1) ($L_{m, S, stellaris} = 90$ cm).

2.3. Standard metabolic rate (SMR)

The care and use of experimental animals complied with French animal welfare laws, guidelines and policies as approved by the Ministry of Higher Education and Research in accordance with the provisions of the French Rural and Maritime Fishing Code, in particular articles R.214-87 to R.214-126 [approval number A3509547].

Twelve eggs were laid in captivity at the marine aquarium of Trégastel from wild females fished in the Bay of Saint Anne (English Channel, France), incubated (~5 months) and bred at the marine station of Dinard until the experiment (~8 months) at 16 ± 1 °C. The juveniles were six males and six females. We included the 12 juveniles in the study to make use of all the hatched individuals, regardless of their sex, considering there was no reproductive investment (i.e., reproductive energy allocation) in the first year. We also captured 12 females using bottom trawl along the Bay of Saint Brieuc (English Channel, France) at the end of May 2023. The 24 individuals were placed in three 700-L biosphere tanks with four juveniles and four captured females per tank. Juveniles were separated from larger individuals to avoid any risk of cannibalism and to ensure optimal feeding, using a crate suspended in the tanks. Sharks were fed *ad libitum* twice a week with thawed hake and squid. Tanks were fully aerated to create a normoxic (>95 % air saturation) environment under each condition with independent filtration systems. Nitrite (< 0.05 mg.L⁻¹) was monitored daily and 1/3 of the tanks' volume was renewed to ensure good water quality, while salinity (34 ppm) and nitrate (< 40 mg.L⁻¹) were monitored weekly.

We chose June temperatures to study standard metabolic rate responses to warm conditions, while ensuring that the temperatures tested were within *S. canicula* current temperature range. As the sea surface temperature at the end of May was around 15 °C at the time of capture, water temperature was progressively increased by 2 °C per week until the desired temperatures were reached ($T_{control} = 15.5$ °C; $T_{SSP2-4.5} = 17.4$ °C; $T_{SSP5-8.5} = 19.5$ °C) and maintained with a heater connected to a temperature control unit. This acclimatisation time also ensured that the individuals caught were in a healthy state before starting the experiment. Individuals were then maintained at the experimental temperatures for a month.

SMRs were determined using intermittent flow static respirometry method, commonly used in elasmobranch species that are capable of buccal pumping (Chen et al., 2008; Molina et al., 2020; Rummer et al., 2022; Sims, 1996). Two homemade transparent respirometers with enrichments were used: 1.5 L for individuals under 28 g and 75 L for individuals over 190 g, and immersed by two in larger mesocosms (reducing individual isolation), with filtered, oxygenated seawater at the same temperature as the stabulation tanks for the duration of the

test, all set in a photo-thermoregulated room with no walk-through. Individuals were fasted for 5 days before oxygen consumption measurements were taken to reach a postabsorptive state for this species (Hopkins and Cech, 1994; Neer et al., 2006; Chen et al., 2008). Individuals were placed in respirometry chambers adapted to their weight, and the first hour was devoted to acclimatisation to the respirometry chamber with a continuous water flow (Tullis and Baillie, 2005; Lear et al., 2018). Then the test alternated between 15 and 60 min of oxygen consumption measurements (depending on the temperature treatment) and 60 min of oxygen renewal. The sharks were then left in the respirometry chambers for 16 h. The time interval between oxygen renewal was long enough for O₂ decline to be detected, but short enough that O₂ levels in the chambers did not fall below 80 % saturation at the end of the measurement period, to avoid stressing individuals (Svendsen et al., 2016). The oxygen saturation was measured using a mini oxygen sensor with a dip probe connected to a Witrox 4 oxygen metre (LoligoSystems). We validated the measurements by following the recommendations of Chabot et al. (2021) and defining a threshold R² of 0.85. Oxygen saturation with empty chambers was measured before and after the respirometry measurements on the sharks and did not reveal any significant microbial respiration rates. As metabolic rates were estimated in relation to the weight of each individual, biometry was carried out after each test. The sharks were individually removed from the respirometry chambers and anaesthetised (benzocaine, 40 mg.L⁻¹ buffered with bicarbonate) for biometry (total length, mass).

The rate of oxygen consumption (mg.O₂.individual⁻¹.h⁻¹) was calculated by multiplying the rate of decrease in oxygen saturation by the volume of the tank (Wheeler et al., 2021). Rates were used to calculate a RQ parameter (approximates the Q10) and converted into g.O₂.g fish⁻¹.day⁻¹ to determine RA and RB parameters (Deslauriers et al., 2017; Figure S2).

2.4. Reproduction

The proportion of mature individuals based on size was converted into the proportion of mature individuals based on weight (Figure S3). The probability of an individual reproducing was determined based on a logistic function that related the fraction of mature individuals at that age to body weight (Ellis and Shackley, 1997; Figure S3). During catsharks peak egg-laying period (1st –30th June) (Ellis and Shackley, 1997), if the random number drawn from a uniform distribution was less than the mature fraction based on an individual's weight each day, then the individual would lay that day (Neer et al., 2007). The number of eggs laid per individual during this period was calculated by multiplying the number of laying events (in days) with a daily egg production rate. The June daily egg production rate of *S. canicula* was determined from Ellis & Shackley (1997) (egg.rate_{S.canicula} = 0.28 egg.day⁻¹.female⁻¹) while that of *S. stellaris* was determined from Capapé et al. (2006) and observations from the Tregastel Aquarium, located in the western part of the English Channel, from 2012 to 2013 (egg.rate_{S.stellaris} = 0.03 egg.day⁻¹.female⁻¹). Reproductive investment was calculated by multiplying the number of eggs laid by the average weight of an egg (egg.weight_{S.canicula} = 4 g; Mellinger, 1983; egg.weight_{S.stellaris} = 17 g; Musa et al., 2018), and subtracting this from the female's weight on June 30th.

2.5. Mortality

The probability of dying was assigned to natural mortality of catsharks ($n = 0.15$) according to the ecopath model of Sánchez et al. (2005) calibrated in the Cantabrian Sea. Mortality was determined by fitting a decreasing curve between annual mortality rate and body weight (Roff, 1993; Cortés, 2004; Figure S4). The Instantaneous annual natural Mortality Rate (IMR) for the smallest individuals of both species was determined for each scenario from the first-year mortality rates determined by Coulon et al. (2024a). These rates were obtained from experiments exposing *S. canicula* embryos and juveniles to historical

temperatures spanning from 1994 to 2015 (AR6 1994–2015), as well as temperatures predicted for the year 2100 under the climate scenarios SSP2–4.5 and SSP5–8.5 ($\text{IMR}_{\text{Age } 0, \text{ control}} = 0.19$; $\text{IMR}_{\text{Age } 0, \text{ SSP2-4.5}} = 0.17$; $\text{IMR}_{\text{Age } 0, \text{ SSP5-8.5}} = 0.89$). The IMR decreases exponentially with weight, approaching 0.15 for the heaviest (oldest) individuals (Sanchez et al., 2005; Figure S4). The maximum age of each species was determined from its growth parameters (i.e., 13 years for *S. canicula* and 16 years for *S. stellaris*). Annual mortality rates were converted to daily rates and if the randomly generated number from a uniform distribution was less than the daily probability of dying, then the individual died and was removed from the simulation.

2.6. Simulation process

The three temperature scenarios (AR6 1994–2015; SSP2–4.5: Middle of the road and SSP5–8.5: Fossil-fuelled Development; Fig. 1) were simulated using the bioenergetic and matrix projection models. All simulations of the bioenergetic model started with 1000 females on the 1st of July. Initial weights for each scenario were generated from a normal distribution based on observed weight-at-birth information of *S. canicula* and *S. stellaris* (Appendix 1). As the *S. stellaris* individuals were not exposed to the experimental conditions, their initial weights for the SSP2–4.5 and SSP5–8.5 scenarios were estimated based on the weight differences observed in *S. canicula* under the same scenarios (Coulon et al., 2024a). Body weight of each individual was updated daily. Weight-dependent maturity was used to determine reproduction (Figure S3). Weight loss associated with laying events was based on the observed average weight of eggs. Numbers of individuals in the cohort were decreased daily on a specified weight-dependent mortality rate (Figure S4). The model predicted the number of individuals alive, average weight of an individual, and number of pups produced by year. These predictions were used to estimate the parameters of age structured matrix projection models.

Weight-age data were transformed into weight-length data using the 'fishR' R package. The predicted length-at-age curves for each scenario were fitted using the nls R function to estimate their parameters (Linf , K , t_0). Subsequently, these growth models were compared using an ANOVA test. The size at maturity (L_m) for each species determined the maturity status of individuals (binomial variable; 0: immature, 1: mature). For each age class, a chi-squared test was conducted to compare the number of mature individuals across scenarios, using maturity as the response variable and scenarios as predictors. The impact of scenarios on offspring production was analysed using a Generalised Linear Model with a Gaussian distribution for *S. canicula* (continuous number of offspring between 0 and 8) and a quasi-binomial distribution with a logit link for *S. stellaris* (continuous number of offspring between 0 and 1).

2.7. Individual-level variability

Two sources of individual variability in the growth of catsharks were simulated. First, individual temperature variability was incorporated to account for the fact that not all individuals are in the same location and therefore experience similar, but not identical, daily temperatures. For each day of the simulation, each individual was assigned a daily water temperature drawn from a normal distribution with the mean equal to the temperature predicted by the temperature function and a standard deviation of the simulated data's variability around the predicted temperatures (Fig. 1). Variability in p values was incorporated to reflect the variability of prey encountered and ingested by individuals depending on their location, as well as variability in prey capture capacity (Neer et al., 2007). Individuals were assigned values of p from a normal distribution having a mean of the age-specific p -value determined through the calibration process, and a coefficient of variation of 1 % (Neer et al., 2007; Table S2).

2.8. Matrix projection models

We used Leslie age-structured matrix projection models to analyse the population-level impacts of warmer water temperature scenarios (Eq. (1)).

$$\begin{pmatrix} 0 & P_0 \cdot m_0 & 0 & \dots & 0 & 0 \\ P_1 & 0 & 0 & \dots & 0 & 0 \\ 0 & P_2 & 0 & \dots & 0 & 0 \\ \vdots & \vdots & \vdots & \ddots & \vdots & \vdots \\ 0 & 0 & 0 & \dots & P_{n-1} & 0 \\ 0 & 0 & 0 & \dots & 0 & 0 \end{pmatrix} \quad (1)$$

The matrix projection models followed females using a birth-pulse structure with a post-breeding census (Caswell, 2000). Annual survival rates (sub-diagonal elements, Table S3) and fertility values, (top row; defined as $f_i = P_i \cdot m_i$ where f_i = fertility at age i , P_i = age-specific survival probability and m_i = age-specific reproductive output, Table S4) of each matrix were estimated from the numbers surviving and pup production (number of pups per female) predicted by the bioenergetics model under the AR6 1994–2015; SSP2–4.5 and SSP5–8.5 scenarios. The age-specific fecundity estimates predicted by the bioenergetics model were divided by 2 to reflect a 1:1 male:female sex ratio.

For each scenario, we calculated the finite (λ) and instantaneous (r) population growth rates, net reproductive rate, and generation time using the 'pop.bio' R package. The finite population growth rate (λ) indicates whether a population is growing ($\lambda > 1$) or declining ($\lambda < 1$) from one period to the next. The instantaneous growth rate (r) is derived from the natural logarithm of λ and reflects the continuous growth rate of the population ($r > 0$ indicates growth; $r < 0$ indicates decline). The net reproductive rate (R_0) represents the average number of offspring produced by each individual over its lifetime, determining whether the population can replace itself. Generation time refers to the average age of parents producing the offspring at stable age distribution.

3. Results

3.1. Bioenergetics model

Model-predicted weights-at-age under the AR6 (1994–2015) scenario closely matched the mean weights from a Von Bertalanffy growth curve and individual measurements derived from observed size-at-age data for both species (ANOVA, $p = 1$; Figure S5, Table S5), indicating that the model predictions are robust.

The bioenergetics model predicts that the number of individuals from the cohort ($N = 1000$) surviving to the first age is markedly lower under the SSP5–8.5 scenario compared to the AR6 1994–2015 and SSP2–4.5 for both species (Fig. 2, Table S3). Survival rates decreased from 80 % and 83 % (Fig. 2) under the AR6 (1994–2015) and SSP2–4.5 scenarios to 33 % for *S. canicula* and 23 % for *S. stellaris* under the SSP5–8.5 (Figure 2; Table S3). Mortality peaks between July and October of age 0 (Figure S6), the first few months of the simulation, when temperatures are the warmest (Fig. 1).

Under the SSP5–8.5 scenario, both *S. canicula* and *S. stellaris* show significant growth differences compared to the AR6 (1994–2015). The average weight of *S. canicula* individuals ranged from 72 % ($W = 18.5 \pm 2.9$ g; $N = 328$) at age 1 to 94 % ($W = 814.8 \pm 150.1$ g; $N = 26$) at age 10, compared to that under the AR6 at similar ages (Table S6). While the weight difference decreased with age in *S. canicula*, no such trend was observed for *S. stellaris* (Fig. 3) where the average weight ranged from 74 % ($W = 39.2 \pm 3.3$ g; $N = 113$) at age 1 to 70 % ($W = 3879.3 \pm 619.3$ g; $N = 67$) at age 14 compared to that under the AR6 (1994–2015) at similar ages (Table S6). Under the SSP2–4.5 scenario, *S. canicula* exhibits growth differences compared to the AR6 (1995–2014), while *S. stellaris* displays only marginal changes. The average weight of *S. canicula* individuals ranged from 95 % ($W = 24.5 \pm 1.6$ g; $N = 837$) at age 1 to 103 % ($W = 887.7 \pm 127.4$ g; $N = 174$) at age 10 compared to that under the

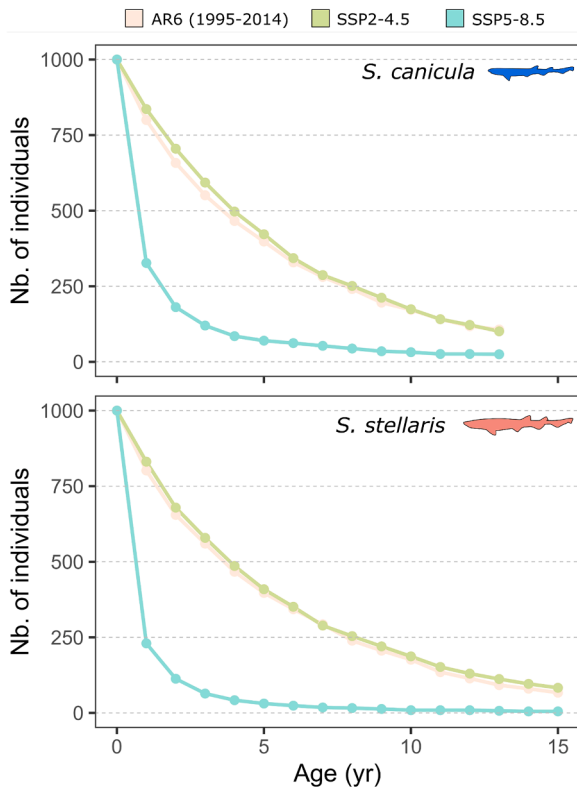


Fig. 2. Predicted survival curves on June 30 of each year. Predicted survival curve under the historical temperatures from 1994 to 2015 (AR6 1994–2015) is shown in beige. Predicted survival curves under the temperatures predicted for 2100 under the climate scenarios SSP2 (Middle of the road) and SSP5 (Fossil-fuelled Development) are respectively shown in light green and light blue. The top panel describes the responses of *S. canicula* (blue shape) and the bottom panel those of *S. stellaris* (light red shape).

AR6 (1994–2015) at similar ages (Table S6) (Fig. 4).

The age at which 50 % of *S. canicula* individuals reach maturity does not differ significantly between scenarios (ranging from 9 to 10 years old). However, maturation occurs slightly later in the youngest age classes under the SSP2–4.5 scenario. This delay is offset by a faster maturation rate in older age classes, resulting in all individuals reaching maturity sooner under SSP2–4.5 than under the AR6 (1994–2015) scenario. Regarding *S. stellaris*, more than half of the individuals reach maturity between ages 9 and 10 under the AR6 (1994–2015) and SSP2–4.5 scenarios. In contrast, under the SSP5–8.5, only 4 out of 1000 individuals from the initial cohort reach maturity at 13 years old.

The maximum number of eggs laid by *S. canicula* in June under the AR6 (1994–2015) scenario is 8.4, whereas it remains below 1 for *S. stellaris* (Fig. 5). In *S. canicula*, egg production by mature individuals is similar between the SSP2–4.5 and AR6 (1994–2015) scenarios, except in the oldest age classes, where it is higher under SSP2–4.5. A similar pattern is observed under SSP5–8.5, although egg production is lower than in AR6 (1994–2015) for the youngest age classes. In *S. stellaris*, no significant difference in egg production is observed between the SSP2–4.5 and AR6 (1994–2015) scenarios. However, under SSP5–8.5, egg production is lower and increasingly variable, mainly due to the very small number of individuals ($N < 10$ from age class 10 onwards).

3.2. Matrix projection model

The population of *S. canicula* is growing steadily ($\lambda = 1.18$; $r = 0.17$), while that of *S. stellaris* remains stable ($\lambda = 0.98 \sim 1$; $r = -0.02 \sim 0$) under the AR6 (1994–2015). Moderately faster individual growth under

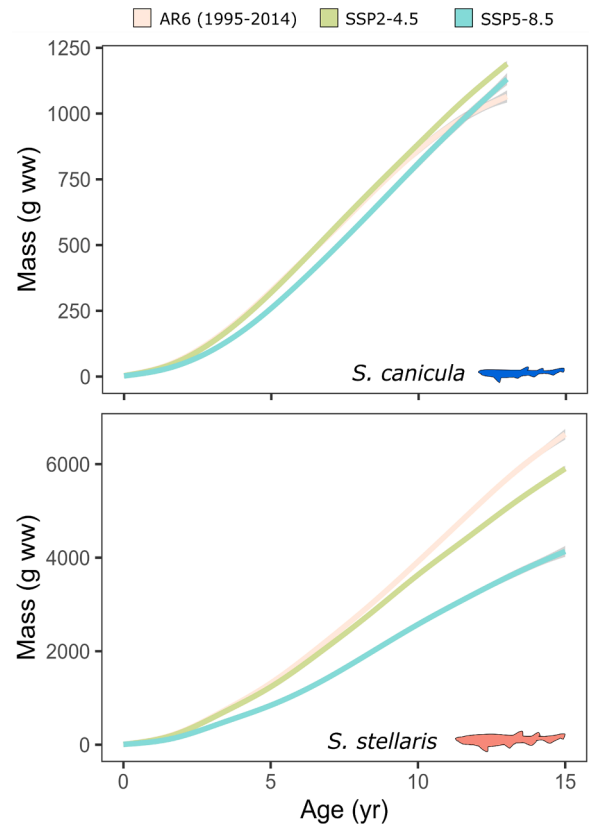


Fig. 3. Predicted average weights (in grams of wet weight, g ww) of all individuals live on June 30 of each year. Predicted average weights curve under the historical temperatures from 1994 to 2015 (AR6 1994–2015) is shown in beige. Predicted average weights under the temperatures predicted for 2100 under the climate scenarios SSP2 (Middle of the road) and SSP5 (Fossil-fuelled Development) are respectively shown in light green and light blue. Uncertainty intervals are represented by shaded regions, corresponding to the 5th and 95th percentiles of the model predictions. The top panel describes the responses of *S. canicula* (blue shape) and the bottom panel those of *S. stellaris* (light red shape).

the SSP2–4.5 scenario resulted in population growth rates, net reproductive rates, and generation times similar to those observed under the AR6 (1994–2015) scenario (Table 2). Conversely, the slower growth of individuals under the SSP5–8.5 scenario, accompanied by changes in reproduction and survival rates, led to a reduced population growth rate, lower reproductive rates, and longer generation times for both species (Table 2). Although there was a sharp decline in egg production in *S. canicula* under the SSP5–8.5 scenario ($R_0 = 1.61$), the finite population rate and instantaneous population growth rate remained positive ($\lambda = 1.09$; $r = 0.09$), indicating a steady population. For *S. stellaris*, the population underwent a marked decline ($\lambda = 0.75$; $r = -0.29$) accompanied by an increase in generation time of 1.22 years.

4. Discussion

We assessed the projected effects of end-of-century sea water temperatures on individual growth, life history traits, and population dynamics of *S. canicula* and *S. stellaris* across SSP2–4.5 and SSP5–8.5 scenarios. Our findings reveal that the moderate warming simulated in SSP2–4.5 exerted discernible impacts on both species at individual and population levels. In contrast, under the more severe warming scenario of SSP5–8.5, we observed pronounced negative effects on the populations of *S. canicula* and *S. stellaris*. Our integration of a bioenergetics model with a matrix projection model provided a robust framework to translate limited physiological information on environmental changes

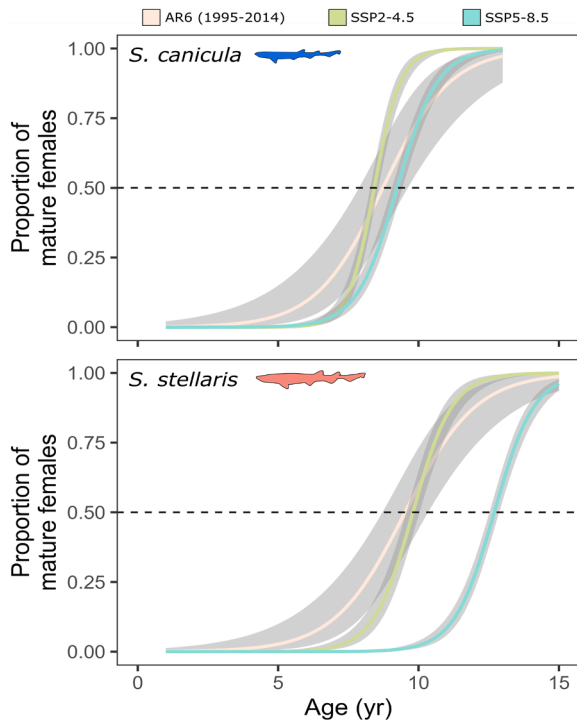


Fig. 4. Predicted percent maturity by age on June 30 of each year. Predicted percent maturity by age under the historical temperatures from 1994 to 2015 (AR6 1994–2015) is shown in beige. Predicted percent maturity by age under the temperatures predicted for 2100 under the climate scenarios SSP2 (Middle of the road) and SSP5 (Fossil-fuelled Development) are respectively shown in light green and light blue. Uncertainty intervals are represented by shaded regions, corresponding to the 5th and 95th percentiles of the model predictions. The top panel describes the responses of *S. canicula* (blue shape) and the bottom panel those of *S. stellaris* (light red shape).

affecting individual growth into meaningful population-level responses for oviparous sharks.

We showed the survival rate of the first-year classes is a critical determinant of the population dynamics of catsharks, as highlighted for several other elasmobranchs previously (e.g., Undulate Ray, *Raja undulata*; Elliott et al., 2020). For the AR6 (1994–2015) and SSP2–4.5 scenarios, the survival rate was relatively high, ranging from 80 % to 83 % for both species. However, under the SSP5–8.5 scenario, the survival rate drastically decreased, dropping to 33 % for *S. canicula* and only 23 % for *S. stellaris*, supporting the vulnerability of oviparous elasmobranch embryos and juveniles to warming temperatures (Coulon et al., 2024a; Musa et al., 2020; Rosa et al., 2014). This finding is particularly concerning given that catsharks produce only a few dozen eggs annually, with *S. stellaris* laying 3 to 6 times fewer eggs than *S. canicula* (Ellis and Shackley, 1997; Pécuchet et al., 2017). Under the SSP5–8.5 scenario, these two species may respond by shifting their spawning areas to deeper waters or migrating to colder regions (Sundby and Nakken, 2008). Between 1997 and 2020, habitat suitability for *S. canicula* increased in the western English Channel, southern and eastern North Sea, while it decreased along the German, Dutch, and Belgian coasts during the summer months (Coulon et al., 2024b). These changes in habitat suitability, particularly during the peak egg-laying period (Ellis and Shackley, 1997), raise the possibility that shifts in coastal spawning areas may already be occurring. Furthermore, it would be interesting to refine species distribution models with the eco-physiological constraints of embryos to provide more accurate maps of suitable spawning habitats. Additionally, species might alter their peak spawning periods to months with milder temperatures, such as spring or late summer (Rogers and Dougherty, 2019; Pankhurst and Munday, 2011). Spatio-temporal monitoring of egg-laying sites could help detect shifts in the species'

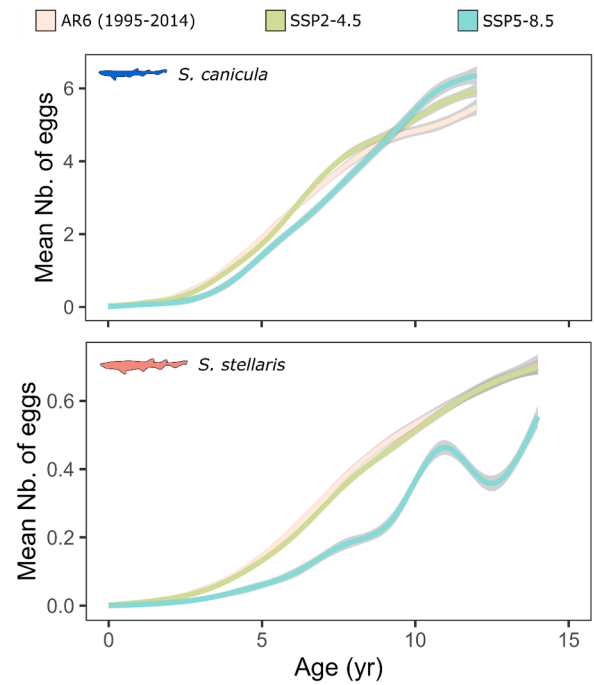



Fig. 5. Predicted June reproductive output by age on June 30 of each year. Predicted reproductive output by age under the historical temperatures from 1994 to 2015 (AR6 1994–2015) is shown in beige. Predicted reproductive output by age under the temperatures predicted for 2100 under the climate scenarios SSP2 (Middle of the road) and SSP5 (Fossil-fuelled Development) are respectively shown in light green and light blue. Uncertainty intervals are represented by shaded regions, corresponding to the 5th and 95th percentiles of the model predictions. The top panel describes the responses of *S. canicula* (blue shape) and the bottom panel those of *S. stellaris* (light red shape).

functional zones rather than focusing solely on suitable habitat, allowing for more effective conservation strategies that address the species dynamic needs. Implementing mobile protection measures could enhance species survival, given the critical role of juvenile survival in the recovery of elasmobranch populations (Ward-Paige et al., 2012). In addition, the lower survival rate of *S. stellaris* compared to *S. canicula* suggests that the early life stages of *S. stellaris* are more sensitive to temperature increases than those of *S. canicula*. While *S. stellaris* is primarily found around the British Isles and lays its eggs in colder waters, *S. canicula* has a broader geographic and environmental range, depositing its eggs across various latitudes and depths (Ellis et al., 2004). This wider distribution is likely to contribute to the observed increased tolerance in the early life stages of *S. canicula*.

The growth rates of surviving *S. canicula* individuals under the AR6 (1994–2015) and SSP2–4.5 scenarios were similar, but they differ significantly from those under the SSP5–8.5 scenario. These differences tended to diminish over time, which may indicate that SSP5–8.5 individuals could compensate for their lower initial growth rates. In this case, it appears that once individuals survive the critical early years, their growth may no longer be threatened by rising temperatures, as is generally observed in fish (Pankhurst and Munday, 2011). In contrast, *S. stellaris* consistently showed lower growth rates at higher temperatures. This suggests that the temperatures encountered by these individuals were no longer optimal for their metabolic functioning. Their energy consumption may be insufficient, or their respiration rate may be excessively high (Scott et al., 2017). Increasing the proportion of ingested energy could compensate for higher metabolic demands (Neer et al., 2007); however, with rising temperatures, access to resources may become less predictable (Brodersen et al., 2011; Lindmark et al., 2022). Furthermore, reducing activity levels could help limit overall energy expenditure (Johansen et al., 2014). However, activity patterns are

Table 2
Finite and instantaneous population growth rates (λ), net reproductive rate, and generation time (yr) calculated from the matrix projection models.

Species	Scenario	Finite population growth rate (λ)	Instantaneous population growth rate (r)	Net reproductive rate (R_0)	Generation time
 <i>S. canicula</i>	AR6 (1994–2015)	1.18	0.17	6.79	8.01
	SSP2–4.5	1.19	0.17	7.00	8.13
	SSP5–8.5	1.09	0.09	1.61	9.39
 <i>S. stellaris</i>	AR6 (1994–2015)	0.98	−0.02	1.47	10.11
	SSP2–4.5	0.98	−0.02	1.48	10.37
	SSP5–8.5	0.75	−0.29	1.02	11.59

directly related to prey encounter rates, the ability to capture prey, and avoid predators. Any reductions in activity are likely to decrease overall foraging success and energy intake, thereby limiting the energy available for growth.

Catsharks’ population growth rates are closely tied to the individuals’ ability to mature. While *S. canicula* females mature first under the AR6 scenario (1994–2015), the proportion of mature individuals increases more rapidly under the SSP2–4.5 scenario. By age 9, more than half of the individuals are mature under both scenarios, with the proportion of mature individuals under the SSP2–4.5 scenario surpassing the AR6 scenario by age 10. Despite a delay, the SSP2–4.5 scenario would favour the maturation of individuals, thereby maintaining a finite population growth rate and generation time comparable to those under the AR6 scenario. Concerning *S. stellaris*, more than half of individuals reach maturity between the ages of 9 and 10 under the AR6 (1994–2015) and SSP2–4.5 scenarios. However, under the SSP5–8.5 scenario, only 4 out of 1000 individuals from the initial cohort reached maturity by the 13th year, posing critical risks to population renewal. Coulon et al. (2024b) observed an increase in habitat suitability for *S. stellaris* between 1997 and 2020 coinciding with rising temperatures, which could suggest favorable conditions for population growth. In our study, the finite population growth rate estimate under AR6 (1994–2015) is <1 (0.98), suggesting that even under historical condition, the population may not have been self-sufficient. On the one hand, density-dependent mechanisms are not explicitly accounted for in our matrix models that do not incorporate feedback mechanisms such as compensatory survival or reproductive adjustments. Therefore, while our projections provide insights into potential population trajectories under different climate scenarios, they do not capture potential buffering effects of density dependence. On the other hand, given the generation time of *S. stellaris*, a 24-year period is likely insufficient to detect significant changes in population structure in Coulon et al. (2024b). As discussed in Coulon et al. (2024b), this apparent increase in habitat suitability may primarily reflect improved identification of *S. stellaris* in scientific bottom trawl surveys rather than a true enhancement of habitat suitability conducive to population growth. Moreover, temperature changes during this period may not yet have driven habitat or population contraction. Nevertheless, in this study, maturation is determined by a threshold of individual length and weight, which was defined as the minimum size observed at fishing markets with an egg emerging from the cloaca. Firstly, we emphasise the age at maturity determined by modelling only partially reflects the age that could be determined by biological observations. Given that *S. stellaris* is a larger species than *S. canicula*, we would expect it to reach maturity at a later age. This strongly supports the need to precisely define the size at maturity for *S. stellaris* and females of many elasmobranchs. This could be achieved through ultrasound scans (Whittamore et al., 2010) conducted during scientific bottom trawl surveys in the Northeast Atlantic (ICES, 2022). Then, predicting maturation and subsequent reproduction based solely on growth may be insufficient. Individuals may have biological age increasing more rapidly in response to increased temperatures, resulting in earlier maturation at smaller sizes and potentially increasing the number of reproductive events in a lifetime (Angiletta,

2004). By comparison, catsharks’ Mediterranean populations exhibit maturation at smaller sizes (Capapé et al., 2006), suggesting that under the SSP5–8.5 scenario, Northeast Atlantic individuals may mature at lower sizes by the end of the century. Additionally, temperature can influence fish maturation independently of warming-induced changes in body growth (Kuparinen et al., 2011; Niu et al., 2023). For instance, experiments with Japanese Medaka (*Oryzias latipes*) have shown that temperature affects both the age and size at maturation, even when growth rates are similar due to varying food levels (Dhillon and Fox, 2004).

The model suggests that some individuals lay eggs before reaching sexual maturity, which is biologically implausible. Therefore, we focus solely on egg production post-maturity. While egg production rates for the oldest age groups of *S. canicula* in the AR6 (1994–2015) and SSP5–8.5 scenarios are similar, in the SSP2–4.5 scenario, higher egg laying was observed at ages 7–12. Daily egg production may increase in response to temperature and mass, as observed in other elasmobranch species such as Thornback Ray (*Raja clavata*), Blonde Ray (*Raja brachyura*), and Spotted Ray (*Raja montagui*), where the highest egg production rates were observed under warmer conditions (Holden et al., 1971). Conversely, increased frequency of egg laying may imply greater energy demand over a given period; thus, maternal investment could be reduced if individuals do not increase their food intake (e.g., by decreasing oocyte diameters; King et al., 2003; McCormick, 1998). For *S. stellaris* both individuals under the SSP2–4.5 and SSP5–8.5 scenarios exhibited lower egg laying rates at various ages (6–14) compared to AR6 (1994–2015). This may indicate that the available resources for individuals are inadequate to support both somatic growth and egg production (Thunell et al., 2023). Furthermore, while the effects of global warming on the reproductive biology of many ectotherms, including teleost fish, are well documented (Alix et al., 2020; Walsh et al., 2019), the impacts on the reproductive biology of elasmobranchs—from gametogenesis to post-zygotic development or pup production, including mate search and gamete storage—are poorly understood. A better understanding of these effects would allow for more accurate population dynamic models that are constrained by species physiology (Horodysky et al., 2015). Furthermore, our bioenergetics models were based on females according to general assumptions; however, the potential effects of temperature on male reproductive biology should not be overlooked (Rankin and Kokko, 2007). For example, mismatches between the reproductive timing of the two sexes (Pratt et al., 2022) or alterations in sperm quantity and quality (Alavi and Cosson, 2005; Wyffels et al., 2020) could cause populations to reach a bottleneck.

Finally, we would like to emphasise that our models were constrained solely by temperature, as the equations calibrating it were temperature-dependent. However, other parameters, such as ocean acidification or deoxygenation, could also significantly impact the survival, growth and reproductive biology of elasmobranchs (Rummer et al., 2022). Acidification may influence elasmobranch behaviour, especially foraging, by modifying the efficiency of energy intake. However, the exact effects of these changes remain unclear. For instance, Port Jackson Shark (*Heterodontus portusjacksoni*) has been observed to take more time to locate food under acidified conditions

(Pistevos et al., 2015), whereas elevated pCO₂ levels do not seem to impact activity levels or foraging behaviour in Epaulette Shark (*Hemiscyllium ocellatum*) (Heinrich et al., 2014). Regarding deoxygenation, a significant concern is that under low oxygen conditions (50 % air saturation), the survival rate of *S. canicula* embryos decreased markedly (Musa et al., 2020), which could further diminish the survival rate of the first age class determined in this study. Integrating these additional environmental factors into future models could provide a more comprehensive understanding of the challenges faced by these species (Koenigstein et al., 2016).

Through the study of *S. canicula* and *S. stellaris*, we demonstrate that populations of a species with later maturity, lower fecundity, and more restricted distribution are more vulnerable to global warming than those of a species with higher fecundity and fewer environmental constraints, highlighting the importance of considering life history traits in conservation strategies. Building on this, and recognizing the impracticality of calibrating a bioenergetics model for each species, we emphasise the urgent need to address the additional pressure of global warming on elasmobranch populations already impacted by human activities.

CRediT authorship contribution statement

Noémie Coulon: Writing – original draft, Visualization, Software, Methodology, Investigation, Funding acquisition, Formal analysis, Conceptualization. **Sophie Elliott:** Writing – original draft, Validation, Supervision, Conceptualization. **Thomas Barreau:** Writing – review & editing, Validation, Resources, Investigation. **Julie Lucas:** Writing – review & editing, Resources, Methodology, Investigation. **Emma Gousset:** Investigation, Formal analysis. **Eric Feunteun:** Writing – review & editing, Supervision, Project administration. **Alexandre Carpentier:** Writing – review & editing, Validation, Supervision, Project administration, Conceptualization.

Declaration of competing interest

The authors declare the following financial interests/personal relationships which may be considered as potential competing interests:

Noémie Coulon reports financial support was provided by Save Our Seas Foundation. If there are other authors, they declare that they have no known competing financial interests or personal relationships that could have appeared to influence the work reported in this paper.

Acknowledgements

This work was funded by the SaveOurSeas Foundation. We would like to thank the Aquarium Marin de Trégastel for its invaluable advice and support. We would also like to thank Pr. Kenneth Rose for his help in understanding bioenergetics, Pr. James Breck for his help in using FishBioenergetics 4.0 and Dr. Kelig Mahé for providing us with supplementary length and weight data for the species studied. We also thank the Elasmobranch-On-Shore observers from the National Museum of Natural History for the data collection. EOS as part of the European Data Collection Framework is co-funded by the European Maritime, Fisheries and Aquaculture Fund and coordinate by the Directorate general for Maritime affairs, Fisheries and Aquaculture (DGAMPA) included into the France's Ministry of the Ecological Transition and Territorial Cohesion. We would also like to thank UMR LIENSs for providing us with equipment to carry out respirometry measurements.

Supplementary materials

Supplementary material associated with this article can be found, in the online version, at [doi:10.1016/j.ecolmodel.2025.111157](https://doi.org/10.1016/j.ecolmodel.2025.111157).

Data availability

I have shared my data and links to my data at the 'Attachment File' step. The length and weight data used for this study are freely available at <https://doi.org/10.1017/S0025315416001752> (Mahé et al., 2018); <https://doi.org/10.1016/j.marenvres.2024.106531> (Coulon et al., 2024a) or in the supplementary data.

References

- Alavi, S., Cosson, J., 2005. Sperm motility in fishes. i. Effects of temperature and pH: a review. *Cell. Biol. Int.* 29 (2), 101–110. <https://doi.org/10.1016/j.cellbi.2004.11.021>.
- Alix, M., Kjesbu, O.S., Anderson, K.C., 2020. From gametogenesis to spawning: How climate-driven warming affects teleost reproductive biology. *J. Fish Biol.* 97 (3), 607–632.
- Angilletta Jr, M.J., Steury, T.D., Sears, M.W., 2004. Temperature, growth rate, and body size in ectotherms: fitting pieces of a life-history puzzle. *Integr. Comp. Biol.* 44 (6), 498–509.
- Bartell, S.M., Breck, J.E., Gardner, R.H., Brenkert, A.L., 1986. Individual parameter perturbation and error analysis of fish bioenergetics models. *Can. J. Fish. Aquat. Sci.* 43 (1), 160–168.
- Baudron, A.R., Needle, C.L., Rijnsdorp, A.D., Tara Marshall, C., 2014. Warming temperatures and smaller body sizes: synchronous changes in growth of North Sea fishes. *Glob. Chang. Biol.* 20 (4), 1023–1031. <https://doi.org/10.1111/gcb.12514>.
- Bohe, J., Labbé, C., 2010. Egg and sperm quality in fish. *Gen. Comp. Endocrinol.* 165 (3), 535–548. <https://doi.org/10.1016/j.ygcen.2009.02.011>.
- Boult, V.L., Quaife, T., Fishlock, V., Moss, C.J., Lee, P.C., Sibly, R.M., 2018. Individual-based modelling of elephant population dynamics using remote sensing to estimate food availability. *Ecol. Modell.* 387, 187–195. <https://doi.org/10.1016/j.ecolmodel.2018.09.010>.
- Boyd, R., Sibly, R., Hyder, K., Walker, N., Thorpe, R., Roy, S., 2020. Simulating the summer feeding distribution of Northeast Atlantic mackerel with a mechanistic individual-based model. *Prog. Ocean.* 183, 102299. <https://doi.org/10.1016/j.pocean.2020.102299>.
- Brodersen, J., Rodriguez-Gil, J.L., Jönsson, M., Hansson, L.-A., Brönmark, C., Nilsson, P. A., Nicolle, A., Berglund, O., 2011. Temperature and resource availability may interactively affect over-wintering success of juvenile fish in a changing climate. *PLoS. ONE*. 6 (10), e24022. <https://doi.org/10.1371/journal.pone.0024022>.
- Brownscombe, J.W., Lawrence, M.J., Deslauriers, D., Filgueira, R., Boyd, R.J., Cooke, S. J., 2022. Applied fish bioenergetics. In: *Fish Physiology Book Series*, 39A. Elsevier Inc, pp. 141–188.
- Bischof, A., Stephan, P., Barreau, T., Bousquet, C., Durieux, É., Elliott, S., Mayot, S., Lapinski, M., Rohr, A., Stephan, É., Bouet, M., Santoni, M.-C., Dorémus, G., Laliche, C., Paillon, C., Coulon, N., Labourgade, P., Carpentier, A., Delesalle, M., & Acou, A. (2024.). *Atlas des chondrichthyens de France métropolitaine—cartographier la présence et la sensibilité des espèces réglementées dans le cadre du programme de mesures D01-PC-OE01-AN1 (sous-action 1) de la DCSMM (Directive cadre stratégie milieu marin) cycle 2*.
- Butler, P.J., & Taylor, E.W. (1975). *The effect of progressive hypoxia on respiration in the dogfish (Scyliorhinus canicula) at different seasonal temperatures*.
- Capapé, C., Vergne, Y., Vianet, R., Guélorget, O., Quignard, J.P., 2006. Biological observations on the nursehound, *Scyliorhinus stellaris* (Linnaeus, 1758) (Chondrichthyes: scyliorhinidae) in captivity. *Acta. Adriat.* 47 (1), 29–36.
- Caswell, H., 2000. *Matrix Population Models*, 1. Sinauer, Sunderland, MA.
- Cerino, D., Overton, A.S., Rice, J.A., Morris, J.A., 2013. Bioenergetics and trophic impacts of the invasive Indo-Pacific lionfish. *Trans. Am. Fish. Soc.* 142 (6), 1522–1534. <https://doi.org/10.1080/00028487.2013.811098>.
- Chabot, D., Zhang, Y., Farrell, A.P., 2021. Valid oxygen uptake measurements: using high r^2 values with good intentions can bias upward the determination of standard metabolic rate. *J. Fish. Biol.* 98 (5), 1206–1216. <https://doi.org/10.1111/jfb.14650>.
- Chen, W.-K., Liu, K.-M., Liao, Y.-Y., 2008. Bioenergetics of juvenile whitespotted bamboo shark *Chiloscyllium plagiosum* [Anonymous (Bennett)]. *J. Fish. Biol.* 72 (6), 1245–1258. <https://doi.org/10.1111/j.1095-8649.2008.01766.x>.
- Christianson, K.R., Johnson, B.M., 2020. Combined effects of early snowmelt and climate warming on mountain lake temperatures and fish energetics. *Arct. Antarct. Alp. Res.* 52 (1), 130–145. <https://doi.org/10.1080/15230430.2020.1741199>.
- Cortés, E., 2004. Life history patterns, demography, and population dynamics. In: Carrier, J.C., Musick, J.A., Heithaus, M.R. (Eds.), *Biology of Sharks and Their Relatives*. CRC Press, Boca Raton, FL, pp. 449–469.
- Coulon, N., Elliott, S., Teichert, N., Auber, A., McLean, M., Barreau, T., Feunteun, E., Carpentier, A., 2024b. Northeast Atlantic elasmobranch community on the move: functional reorganization in response to climate change. *Glob. Chang. Biol.* 30 (1), e17157. <https://doi.org/10.1111/gcb.17157>.
- Coulon, N., Lindegren, M., Goberville, E., Toussaint, A., Receveur, A., Auber, A., 2023. Threatened fish species in the Northeast Atlantic are functionally rare. *Glob. Ecol. Biogeogr.* 32 (10), 1827–1845. <https://doi.org/10.1111/geb.13731>.
- Coulon, N., Pilet, S., Lizé, A., Lacoue-Labarthe, T., Sturbois, A., Toussaint, A., Feunteun, E., Carpentier, A., 2024a. Shark critical life stage vulnerability to monthly temperature variations under climate change. *Mar. Env. Res.* 198, 106531. <https://doi.org/10.1016/j.marenvres.2024.106531>.
- Deslauriers, D., Chipps, S.R., Breck, J.E., Rice, J.A., Madenjian, C.P., 2017. Fish bioenergetics 4.0: an R-based modeling application. *Fisheries*. 42 (11), 586–596.

- Dhillon, R.S., Fox, M.G., 2004. Growth-independent effects of temperature on age and size at maturity in Japanese Medaka (*Oryzias latipes*). *Copeia*. (1), 37–45. <https://doi.org/10.1643/Ci-02-098R1>. 2004.
- Donelson, J., Munday, P., McCormick, M., Pankhurst, N., Pankhurst, P., 2010. Effects of elevated water temperature and food availability on the reproductive performance of a coral reef fish. *Mar. Ecol. Prog. Ser.* 401, 233–243. <https://doi.org/10.3354/meps08366>.
- Dulvy, N.K., Rogers, S.I., Jennings, S., Stelzenmiller, V., Dye, S.R., Skjoldal, H.R., 2008. Climate change and deepening of the North Sea fish assemblage: a biotic indicator of warming seas. *J. Appl. Ecol.* 45 (4), 1029–1039. <https://doi.org/10.1111/j.1365-2664.2008.01488.x>.
- D. Rankin, J., Kokko, H., 2007. Do males matter? The role of males in population dynamics *Oikos*. 116 (2), 335–348. <https://doi.org/10.1111/j.0030-1299.2007.15451.x>.
- Duncan, M.I., James, N.C., Potts, W.M., Bates, A.E., 2020. Different drivers, common mechanism: the distribution of a reef fish is restricted by local-scale oxygen and temperature constraints on aerobic metabolism. *Conserv. Physiol.* 8 (1), coaa090. <https://doi.org/10.1093/conphys/coaa090>.
- Elliott, S.A.M., Carpentier, A., Feunteun, E., Trancart, T., 2020. Distribution and life history trait models indicate vulnerability of skates. *Prog. Ocean.* 181, 102256. <https://doi.org/10.1016/j.pocean.2019.102256>.
- Ellis, J.R., Cruz-Martínez, A., Rackham, B.D., Rogers, S.I., 2004. The distribution of chondrichthyan fishes around the British Isles and implications for conservation. *J. Northwest Atl. Fish. Sci.* 35, 195–213. <https://doi.org/10.2960/J.v35.m485>.
- Ellis, J.R., Shackley, S.E., 1997. The reproductive biology of *scyliorhinus canicula* in the Bristol Channel, U.K. *J. Fish. Biol.* 51 (2), 361–372. <https://doi.org/10.1111/j.1095-8649.1997.tb01672.x>.
- Finucci, B., Derrick, D., Pacoureau, N., 2021. *Scyliorhinus Stellaris*. The IUCN Red List of Threatened Species, 2021e. T161484A124493465.
- Fricker, O., Havlik, P., Rogelj, J., Klimont, Z., Gusti, M., Johnson, N., Kolp, P., Strubecker, M., Valin, H., Amann, M., Ermolova, T., Forsell, N., Herrero, M., Heyes, C., Kindermann, G., Krey, V., McCollum, D.L., Obersteiner, M., Pachauri, S., Riahi, K., 2017. The marker quantification of the Shared Socioeconomic Pathway 2: a middle-of-the-road scenario for the 21st century. *Glob. Environ. Change*. 42, 251–267. <https://doi.org/10.1016/j.gloenvcha.2016.06.004>.
- Greenstreet, S.P.R., Fraser, H.M., Rogers, S.I., Trenkel, V.M., Simpson, S.D., Pinnegar, J. K., 2012. Redundancy in metrics describing the composition, structure, and functioning of the North Sea demersal fish community. *ICES. J. Mar. Sci.* 69 (1), 8–22. <https://doi.org/10.1093/icesjms/fsr188>.
- Gutiérrez, J.M., R.G. Jones, G.T. Narisma, L.M. Alves, M. Amjad, I.V. Gorodetskaya, M. Grose, N.A.B. Klutse, S. Krakovska, J. Li, D. Martínez-Castro, L.O. Mearns, S.H. Mernild, T. Ngo-Duc, B. van den Hurk, and J.-H. Yoon, 2021. Atlas. In Climate change 2021: the physical science basis. Contribution of Working Group I to the Sixth Assessment Report of the Intergovernmental Panel On Climate Change [Masson-Delmotte, V., P. Zhai, A. Pirani, S.L. Connors, C. Péan, S. Berger, N. Caud, Y. Chen, L. Goldfarb, M.I. Gomis, M. Huang, K. Leitzell, E. Lonnoy, J.B.R. Matthews, T. K. Maycock, T. Waterfield, O. Yelekçi, R. Yu, and B. Zhou (eds.)]. Cambridge University Press. In Press. Interactive Atlas available from <http://interactive-atlas.ipcc.ch/2025>.
- Hanson, P.C., Johnson, T.B., Schindler, D.E., Kitchell, J.F., 1997. Fish Bioenergetics 3.0 Software For Windows. University of Wisconsin Center for Limnology, Sea Grant Institute, p. 116. Technical Report WISCU-T-97-001.
- Hartman, K.J., Jensen, O.P., 2017. Anticipating climate change impacts on Mongolian salmonids: bioenergetics models for lenok and Baikal grayling. *Ecol. Freshw. Fish.* 26 (3), 383–396. <https://doi.org/10.1111/eff.12282>.
- Heinrich, D.D.U., Rummer, J.L., Morash, A.J., Watson, S.-A., Simpfendorfer, C.A., Heupel, M.R., Munday, P.L., 2014. A product of its environment: the epaulette shark (*Hemiscyllium ocellatum*) exhibits physiological tolerance to elevated environmental CO₂. *Conserv. Physiol.* 2 (1). <https://doi.org/10.1093/conphys/cou047> cou047–cou047.
- Holden, M.J., Rout, D.W., Humphreys, C.N., 1971. The rate of egg laying by three species of ray. *ICES. J. Mar. Sci.* 33 (3), 335–339. <https://doi.org/10.1093/icesjms/33.3.335>.
- Holsman, K.K., Aydin, K., Sullivan, J., Hurst, T., Kruse, G.H., 2019. Climate effects and bottom-up controls on growth and size-at-age of Pacific halibut (*Hippoglossus stenolepis*) in Alaska (USA). *Fish. Ocean.* 28 (3), 345–358. <https://doi.org/10.1111/fog.12416>.
- Holt, R.E., Jørgensen, C., 2015. Climate change in fish: effects of respiratory constraints on optimal life history and behaviour. *Biol. Lett.* 11 (2), 20141032. <https://doi.org/10.1098/rsbl.2014.1032>.
- Hopkins, T.E., Cech, J.J., 1994. Effect of temperature on oxygen consumption of the bat ray, *Myliobatis californica* (Chondrichthyes, Myliobatidae). *Copeia*. (2), 529–532. 1994.
- Horodysky, A.Z., Cooke, S.J., Brill, R.W., 2015. Physiology in the service of fisheries science: why thinking mechanistically matters. *Rev. Fish Biol. Fish.* 25 (3), 425–447. <https://doi.org/10.1007/s11160-015-9393-y>.
- Huss, M., Lindmark, M., Jacobson, P., Van Dorst, R.M., Gårdmark, A., 2019. Experimental evidence of gradual size-dependent shifts in body size and growth of fish in response to warming. *Glob. Chang. Biol.* 25 (7), 2285–2295. <https://doi.org/10.1111/gcb.14637>.
- ICES. 2022. International bottom trawl survey working group (IBTSWG). ICES Scientific Reports. 04:65. 183pp. <http://doi.org/10.17895/ices.pub.20502828>.
- Iturbide, M., Fernández, J., Gutiérrez, J.M., Bedia, J., Cimadevilla, E., Díez-Sierra, J., Manzanar, R., Casanueva, A., Baño-Medina, J., Milovac, J., Herrera, S., Cofiño, A.S., San Martín, D., García-Díez, M., Hauser, M., Huard, D., Yelekçi, Ö., 2021. Repository supporting the implementation of FAIR principles in the IPCC-WG1 Atlas. Zenodo. <https://doi.org/10.5281/zenodo.3691645>. Available from: <https://github.com/IPCC-WG1Atlas>.
- Ivory, P., Jeal, F., Nolan, C.P., 2004. Age determination, growth and reproduction in the lesser-spotted dogfish, *scyliorhinus canicula* (L.). *J. Northwest Atl. Fish. Sci.* 35, 89–106. <https://doi.org/10.2960/J.v35.m504>.
- IPCC, 2021: Climate Change 2021: the physical science basis. Contribution of Working Group I to the Sixth Assessment Report of the Intergovernmental Panel On Climate Change [Masson-Delmotte, V., P. Zhai, A. Pirani, S.L. Connors, C. Péan, S. Berger, N. Caud, Y. Chen, L. Goldfarb, M.I. Gomis, M. Huang, K. Leitzell, E. Lonnoy, J.B.R. Matthews, T.K. Maycock, T. Waterfield, O. Yelekçi, R. Yu, and B. Zhou (eds.)]. Cambridge University Press, Cambridge, United Kingdom and New York, NY, USA, In press. <https://doi.org/10.1017/9781009157896>.
- Johansen, J.L., Messmer, V., Coker, D.J., Hoey, A.S., Pratchett, M.S., 2014. Increasing ocean temperatures reduce activity patterns of a large commercially important coral reef fish. *Glob. Chang. Biol.* 20 (4), 1067–1074. <https://doi.org/10.1111/gcb.12452>.
- King, H.R., Pankhurst, N.W., Watts, M., Pankhurst, P.M., 2003. Effect of elevated summer temperatures on gonadal steroid production, vitellogenesis and egg quality in female Atlantic salmon. *J. Fish. Biol.* 63 (1), 153–167. <https://doi.org/10.1046/j.1095-8649.2003.00137.x>.
- Kitchell, J.F., Koonce, J.F., Magnuson, J.J., O'Neill, R.V., Shugart Jr, H.H., Booth, R.S., 1974. Model of fish biomass dynamics. *Trans. Am. Fish. Soc.* 103 (4), 786–798.
- Kitchell, J.F., Stewart, D.J., Weininger, D., 1977. Applications of a bioenergetics model to yellow perch (*Perca flavescens*) and walleye (*Stizostedion vitreum vitreum*). *J. Fish. Board Can.* 34 (10), 1922–1935.
- Koenigstein, S., Mark, F.C., Gößling-Reisemann, S., Reuter, H., Poertner, H.-O., 2016. Modelling climate change impacts on marine fish populations: process-based integration of ocean warming, acidification and other environmental drivers. *Fish. Fish.* 17 (4), 972–1004. <https://doi.org/10.1111/faf.12155>.
- Kooijman, S.A.L.M., 2010. Dynamic Energy Budget Theory For Metabolic Organisation. Cambridge university press.
- Krieger, E., Bauer, N., Popp, A., Humpenöder, F., Leimbach, M., Strefler, J., Baumstark, L., Bodirsky, B.L., Hilaire, J., Klein, D., Mouratiadou, I., Weindl, I., Bertram, C., Dietrich, J.-P., Luderer, G., Pehl, M., Pietzcker, R., Piontek, F., Lotze-Campen, H., Edenhofer, O., 2017. Fossil-fueled development (SSP5): an energy and resource intensive scenario for the 21st century. *Glob. Environ. Change*. 42, 297–315. <https://doi.org/10.1016/j.gloenvcha.2016.05.015>.
- Kuparinen, A., Cano, J.M., Loehr, J., Herczeg, G., Gonda, G., Merilä, J., 2011. Fish age at maturation is influenced by temperature independently of growth. *Oecologia*. 167 (2), 435–443. <https://doi.org/10.1007/s00442-011-1989-x>.
- Lear, K.O., Gleiss, A.C., Whitney, N.M., 2018. Metabolic rates and the energetic cost of external tag attachment in juvenile blacktip sharks *Carcharhinus limbatus*. *J. Fish. Biol.* 93 (2), 391–395. <https://doi.org/10.1111/jfb.13663>.
- Lear, K.O., Morgan, D.L., Whitty, J.M., Whitney, N.M., Byrnes, E.E., Beatty, S.J., Gleiss, A.C., 2020. Divergent field metabolic rates highlight the challenges of increasing temperatures and energy limitation in aquatic ectotherms. *Oecologia*. 193 (2), 311–323. <https://doi.org/10.1007/s00442-020-04669-x>.
- Lefevre, S., Wang, T., McKenzie, D.J., 2021. The role of mechanistic physiology in investigating impacts of global warming on fishes. *J. Exp. Biol.* 224 (Suppl_1), jeb238840. <https://doi.org/10.1242/jeb.238840>.
- Lindmark, M., Audzijonyte, A., Blanchard, J.L., Gårdmark, A., 2022. Temperature impacts on fish physiology and resource abundance lead to faster growth but smaller fish sizes and yields under warming. *Glob. Chang. Biol.* 28 (21), 6239–6253. <https://doi.org/10.1111/gcb.16341>.
- Little, A.G., Loughland, I., Seebacher, F., 2020. What do warming waters mean for fish physiology and fisheries? *J. Fish. Biol.* 97 (2), 328–340. <https://doi.org/10.1111/jfb.14402>.
- Madeira, D., Costa, P.M., Vinagre, C., Diniz, M.S., 2016. When warming hits harder: survival, cellular stress and thermal limits of *Sparus aurata* larvae under global change. *Mar. Biol.* 163 (4), 91. <https://doi.org/10.1007/s00227-016-2856-4>.
- Mahé, K., Bellamy, E., Delpech, J.P., Lazard, C., Salaun, M., Vérin, Y., Coppin, F., Travers-Trolet, M., 2018. Evidence of a relationship between weight and total length of marine fish in the North-eastern Atlantic Ocean: physiological, spatial and temporal variations. *J. Mar. Biol. Assoc. U. K.* 98 (3), 617–625. <https://doi.org/10.1017/S0025315416001752>.
- McCormick, M.I., 1998. Behaviorally induced maternal stress in a fish influences progeny quality by a hormonal mechanism. *Ecology*. 79 (6), 1873–1883. [https://doi.org/10.1890/0012-9658\(1998\)079\[1873:BIMSIA\]2.0.CO;2](https://doi.org/10.1890/0012-9658(1998)079[1873:BIMSIA]2.0.CO;2).
- Molina, J.M., Finotto, L., Walker, T.I., Reina, R.D., 2020. The effect of gillnet capture on the metabolic rate of two shark species with contrasting lifestyles. *J. Exp. Mar. Biol. Ecol.* 526, 151354. <https://doi.org/10.1016/j.jembe.2020.151354>.
- Munday, P.L., Jones, G.P., Pratchett, M.S., Williams, A.J., 2008. Climate change and the future for coral reef fishes. *Fish. Fish.* 9 (3), 261–285. <https://doi.org/10.1111/j.1467-2979.2008.00281.x>.
- Musa, S.M., Czachur, M.V., Shiels, H.A., 2018. Oviparous elasmobranch development inside the egg case in 7 key stages. *PLOS. ONE*. 13 (11), e0206984. <https://doi.org/10.1371/journal.pone.0206984>.
- Musa, S.M., Ripley, D.M., Moritz, T., Shiels, H.A., 2020. OCEAN WARMING AND HYPOXIA AFFECT EMBRYONIC GROWTH, FITNESS AND SURVIVAL OF SMALL-SPOTTED CATSHARKS, *scyliorhinus canicula*. *J. Fish. Biol.* 97 (1), 257–264. <https://doi.org/10.1111/jfb.14370>.
- Neer, J.A., Carlson, J.K., Thompson, B.A., 2006. Standard oxygen consumption of seasonally acclimatized cownose rays, *Rhinoptera bonasus* (Mitchill 1815), in the northern Gulf of Mexico. *Fish. Physiol. Biochem.* 32, 67–71.
- Neer, J., Rose, K., Cortés, E., 2007. Simulating the effects of temperature on individual and population growth of *Rhinoptera bonasus*: a coupled bioenergetics and matrix modeling approach. *Mar. Ecol. Prog. Ser.* 329, 211–223. <https://doi.org/10.3354/meps329211>.

- Niu, J., Huss, M., Vasemägi, A., Gårdmark, A., 2023. Decades of warming alters maturation and reproductive investment in fish. *Ecosphere*. 14 (1), e4381. <https://doi.org/10.1002/ecs2.4381>.
- OBIS, 2023. Ocean Biodiversity Information System. Intergovernmental Oceanographic Commission of UNESCO. <https://obis.org>.
- Otero, J., Jensen, A.J., L'Abée-Lund, J.H., Stenseth, N.C., Størvik, G.O., Vøllestad, L.A., 2012. Contemporary ocean warming and freshwater conditions are related to later sea age at maturity in Atlantic salmon spawning in Norwegian rivers. *Ecol. Evol.* 2 (9), 2192–2203. <https://doi.org/10.1002/ece3.337>.
- Pankhurst, N.W., Munday, P.L., 2011. Effects of climate change on fish reproduction and early life history stages. *Mar. Freshw. Res.* 62 (9), 1015. <https://doi.org/10.1071/MF10269>.
- Pankhurst, N.W., Purser, G.J., Van Der Kraak, G., Thomas, P.M., Forteach, G.N.R., 1996. Effect of holding temperature on ovulation, egg fertility, plasma levels of reproductive hormones and in vitro ovarian steroidogenesis in the rainbow trout *Oncorhynchus mykiss*. *Aquaculture*. 146 (3–4), 277–290. [https://doi.org/10.1016/S0044-8486\(96\)01374-9](https://doi.org/10.1016/S0044-8486(96)01374-9).
- Payne, N.L., Smith, J.A., Van Der Meulen, D.E., Taylor, M.D., Watanabe, Y.Y., Takahashi, A., Marzullo, T.A., Gray, C.A., Cadiou, G., Suthers, I.M., 2016. Temperature dependence of fish performance in the wild: links with species biogeography and physiological thermal tolerance. *Funct. Ecol.* 30 (6), 903–912. <https://doi.org/10.1111/1365-2435.12618>.
- Pecuchet, L., Lindegren, M., Hidalgo, M., Delgado, M., Esteban, A., Fock, H.O., Gil De Sola, L., Punzón, A., Sölmundsson, J., Payne, M.R., 2017. From traits to life-history strategies: deconstructing fish community composition across European seas. *Glob. Ecol. Biogeogr.* 26 (7), 812–822. <https://doi.org/10.1111/geb.12587>.
- Piiper, J., Meyer, M., Worth, H., Willmer, H., 1977. Respiration and circulation during swimming activity in the dogfish *Scyliorhinus stellaris*. *Respir. Physiol.* 30 (1–2), 221–239.
- Pistevos, J.C.A., Nagelkerken, I., Rossi, T., Olmos, M., Connell, S.D., 2015. Ocean acidification and global warming impair shark hunting behaviour and growth. *Sci. Rep.* 5 (1), 16293. <https://doi.org/10.1038/srep16293>.
- Politikos, D., Somarakis, S., Tsiaras, K.P., Giannoulaki, M., Petihakis, G., Machias, A., Triantafyllou, G., 2015a. Simulating anchovy's full life cycle in the northern Aegean Sea (eastern Mediterranean): a coupled hydro-biogeochemical-IBM model. *Prog. Ocean.* 138, 399–416. <https://doi.org/10.1016/j.pcean.2014.09.002>.
- Politikos, D.V., Huret, M., Petitgas, P., 2015b. A coupled movement and bioenergetics model to explore the spawning migration of anchovy in the Bay of Biscay. *Ecol. Modell.* 313, 212–222. <https://doi.org/10.1016/j.ecolmodel.2015.06.036>.
- Pratt, H.L., Pratt, T.C., Knotek, R.J., Carrier, J.C., Whitney, N.M., 2022. Long-term use of a shark breeding ground: three decades of mating site fidelity in the nurse shark, *Ginglymostoma cirratum*. *PLOS ONE*. 17 (10), e0275323. <https://doi.org/10.1371/journal.pone.0275323>.
- Rice, J.A., Cochran, P.A., 1984. Independent evaluation of a bioenergetics model for largemouth bass. *Ecology*. 65 (3), 732–739.
- Roff, D., 1993. *Evolution of Life histories: Theory and Analysis*. Springer Science & Business Media.
- Rogers, L.A., Dougherty, A.B., 2019. Effects of climate and demography on reproductive phenology of a harvested marine fish population. *Glob. Chang. Biol.* 25 (2), 708–720. <https://doi.org/10.1111/gcb.14483>.
- Rosa, R., Baptista, M., Lopes, V.M., Pegado, M.R., Ricardo Paula, J., Trübenbach, K., Leal, M.C., Calado, R., Repolho, T., 2014. Early-life exposure to climate change impairs tropical shark survival. *Proc. R. Soc. B: Biol. Sci.* 281 (1793), 20141738. <https://doi.org/10.1098/rspb.2014.1738>.
- Rousseau, Y., Watson, R.A., Blanchard, J.L., Fulton, E.A., 2019. Evolution of global marine fishing fleets and the response of fished resources. *Proc. Natl. Acad. Sci.* 116 (25), 12238–12243. <https://doi.org/10.1073/pnas.1820344116>.
- Rummer, J.L., Bouyoucos, I.A., Wheeler, C.R., Pereira Santos, C., Rosa, R., 2022. In: Carrier, J.C., Simpfendorfer, C.A., Heithaus, M.R., Yopak, K.E. (Eds.), Chapter 25: Biology of Sharks and Their Relatives, 3rd ed. CRC Press. Climate Change and Sharks. <https://doi.org/10.1201/9781003262190>.
- Sánchez, F., Rodríguez-Cabello, C., Olaso, I., 2005. The role of elasmobranchs in the Cantabrian Sea Shelf ecosystem and impact of the fisheries on them. *J. Northwest Atl. Fish. Sci.* 35, 467–480. <https://doi.org/10.2960/J.v35.m496>.
- Schulte, P.M., 2015. The effects of temperature on aerobic metabolism: towards a mechanistic understanding of the responses of ectotherms to a changing environment. *J. Exp. Biol.* 218 (12), 1856–1866. <https://doi.org/10.1242/jeb.118851>.
- Scott, M., Heupel, M., Tobin, A., Pratchett, M., 2017. A large predatory reef fish species moderates feeding and activity patterns in response to seasonal and latitudinal temperature variation. *Sci. Rep.* 7 (1), 12966. <https://doi.org/10.1038/s41598-017-13277-4>.
- Sguotti, C., Lynam, C.P., García-Carreras, B., Ellis, J.R., Engelhard, G.H., 2016. Distribution of skates and sharks in the North Sea: 112 years of change. *Glob. Chang. Biol.* 22 (8), 2729–2743. <https://doi.org/10.1111/gcb.13316>.
- Shapiro Goldberg, D., Van Rijn, I., Kiflawi, M., Belmaker, J., 2019. Decreases in length at maturation of Mediterranean fishes associated with higher sea temperatures. *ICES J. Mar. Sci.* 76 (4), 946–959. <https://doi.org/10.1093/icesjms/fsz011>.
- Sibly, R.M., Grimm, V., Martin, B.T., Johnston, A.S.A., Kulakowska, K., Topping, C.J., Calow, P., Nabe-Nielsen, J., Thorbek, P., DeAngelis, D.L., 2013. Representing the acquisition and use of energy by individuals in agent-based models of animal populations. *Method. Ecol. Evol.* 4 (2), 151–161. <https://doi.org/10.1111/2041-210x.12002>.
- Simon, A., Poppeschi, C., Plecha, S., Charria, G., Russo, A., 2023. *Coastal and Regional Marine Heatwaves and Cold-Spells in the Northeast Atlantic* [Preprint]. situ Observations/Air-sea fluxes/Surface/Shelf Seas/Ocean-shelf interactions. <https://doi.org/10.5194/egusphere-2023-430>.
- Sims, D.W., 1996. The effect of body size on the standard metabolic rate of the lesser spotted dogfish. *J. Fish. Biol.* 48 (3), 542–544. <https://doi.org/10.1111/j.1095-8649.1996.tb01447.x>.
- Sims, D.W., Davies, S.J., 1994. Does specific dynamic action (SDA) regulate return of appetite in the lesser spotted dogfish, *scyliorhinus canicula*? *J. Fish. Biol.* 45 (2), 341–348. <https://doi.org/10.1111/j.1095-8649.1994.tb01313.x>.
- Sims, D.W., Wearmouth, V.J., Southall, E.J., Hill, J.M., Moore, P., Rawlinson, K., Hutchinson, N., Budd, G.C., Righton, D., Metcalfe, J.D., Nash, J.P., Morritt, D., 2006. Hunt warm, rest cool: bioenergetic strategy underlying diel vertical migration of a benthic shark. *J. Anim. Ecol.* 75 (1), 176–190. <https://doi.org/10.1111/j.1365-2656.2005.01033.x>.
- Smith, A.D.M., Garcia, S.M., 2014. Fishery management: contrasts in the Mediterranean and the Atlantic. *Curr. Biol.* 24 (17), R810–R812. <https://doi.org/10.1016/j.cub.2014.07.031>.
- Sundby, S., Nakken, O., 2008. Spatial shifts in spawning habitats of Arcto-Norwegian cod related to multidecadal climate oscillations and climate change. *ICES J. Mar. Sci.* 65 (6), 953–962. <https://doi.org/10.1093/icesjms/fsn085>.
- Svendsen, M.B.S., Bushnell, P.G., Steffensen, J.F., 2016. Design and setup of intermittent-flow respirometry system for aquatic organisms. *J. Fish. Biol.* 88 (1), 26–50. <https://doi.org/10.1111/jfb.12797>.
- Thunell, V., Gårdmark, A., Huss, M., Vindenes, Y., 2023. Optimal energy allocation trade-off driven by size-dependent physiological and demographic responses to warming. *Ecology*. 104 (4), e3967. <https://doi.org/10.1002/ecy.3967>.
- Thornton, K.W., Lessem, A.S., 1978. A temperature algorithm for modifying biological rates. *Trans. Am. Fish. Soc.* 107 (2), 284–287.
- Tullis, A., Baillie, M., 2005. The metabolic and biochemical responses of tropical whitespotted bamboo shark *Chiloscyllium plagiosum* to alterations in environmental temperature. *J. Fish. Biol.* 67 (4), 950–968. <https://doi.org/10.1111/j.0022-1112.2005.00795.x>.
- Walls, R.H.L., Dulvy, N.K., 2021. Tracking the rising extinction risk of sharks and rays in the Northeast Atlantic Ocean and Mediterranean Sea. *Sci. Rep.* 11 (1), 15397. <https://doi.org/10.1038/s41598-021-94632-4>.
- Walsh, B.S., Parratt, S.R., Hoffmann, A.A., Atkinson, D., Snook, R.R., Bretman, A., Price, T.A.R., 2019. The impact of climate change on fertility. *Trends. Ecol. Evol.* (Amst.) 34 (3), 249–259. <https://doi.org/10.1016/j.tree.2018.12.002>.
- Ward-Paige, C.A., Keith, D.M., Worm, B., Lotze, H.K., 2012. Recovery potential and conservation options for elasmobranchs. *J. Fish Biol.* 80 (5), 1844–1869.
- Wheeler, C.R., Rummer, J.L., Bailey, B., Lockwood, J., Vance, S., Mandelman, J.W., 2021. Future thermal regimes for epaulette sharks (*Hemiscyllium ocellatum*): growth and metabolic performance cease to be optimal. *Sci. Rep.* 11 (1), 454. <https://doi.org/10.1038/s41598-020-79953-0>.
- Whittamore, J.M., Bloomer, C., Hanna, G.M., McCarthy, I.D., 2010. Evaluating ultrasonography as a non-lethal method for the assessment of maturity in oviparous elasmobranchs. *Mar. Biol.* 157, 2613–2624.
- Winberg, G.G., 1956. Rate of metabolism and food requirements of fishes. *Fish. Res. Bd. Can. Trans. Ser.* 433, 1–251.
- Wyffels, J.T., George, R., Adams, L., Adams, C., Clauss, T., Newton, A., Hyatt, M.W., Yach, C., Penfold, L.M., 2020. Testosterone and semen seasonality for the sand tiger shark *Carcharias taurus*. *Biol. Reprod.* 102 (4), 876–887. <https://doi.org/10.1093/biolre/iox221>.